2526 © *1990 The Chemical Society of Japan* *Bull. Chem. Soc. Jpn.,* ***63,*** *2526—2530 (1990)* [Vol. 63, No. 9

A New Apparatus for Simultaneous Measurement of Acoustic Emission and Differential Thermal Analysis and Its Application to Dehydration, Phase Transition, and Decomposition Studies of Several Inorganic Salts

Shiro SHIMADA* and Ryusaburo FURUICHI†
Department of Applied Chemistry, Faculty of Engineering,
Hokkaido University, Sapporo 060
†Analytical Chemistry Laboratory, Faculty of Engineering,
Hokkaido University, Sapporo 060
(Received March 17, 1990)

A new apparatus for simultaneous measurements of acoustic emission (AE) and differential thermal analysis (DTA) is described. Two fused silica cells are used as the sample and reference holders and a fused silica rod, fixed at the bottom of the sample holder, acts as the waveguide for AE signals emitted in the sample. A 140 KHz resonance frequency sensor is attached at the end of the rod to detect the AE signals which are converted by an AE tester to three parameters, the wave form, the event count rate, and the cumulative count. The technique has been successfully utilized to study the dehydration, phase transition, and decomposition of NaN_3, KNO_3, $KClO_4$, $CaCrO_4 \cdot 0.1H_2O$, and $MgCl_2 \cdot 6H_2O$, for which the interesting results are reported.

It has been known for many years that when a solid is subjected to certain levels of stress, discrete acoustic wave packets are generated.[1] The phenomenon of such sound generation in materials is termed acoustic emission (AE). When a mechanical event such as occurrence and propagation of cracks, accumulation of stress, or movement of dislocation takes place in a solid, AE waves are emitted from the solid. Where the mechanical event is caused by a thermochemical process such as decomposition, dehydration, or phase transition of a solid, AE waves should be generated from the solid in the course of the process. Thus, if the acoustic emission technique is used as a thermoanalytical method, it provides a unique information about the thermal process which is not obtained from conventional thermal analysis. The pioneering studies of the thermal process using the AE technique were carried out by Lønvik,[2] who reported the phenomenological behavior of thermal decomposition and phase transition in several minerals.

The present authors have designed a new apparatus for acoustic emission thermal analysis which simultaneously permits the measurement of differential thermal analysis (DTA), and have reported briefly on its application to the thermal decomposition of $KClO_4$ and $NaClO_4$.[3] This paper describes in detail the new apparatus for the simultaneous AE and DTA technique and the results obtained by its successful application to the dehydration, phase transition, decomposition, and melting of the inorganic salts such as NaN_3, KNO_3, $CaCrO_4 \cdot 0.1H_2O$, $MgCl_2 \cdot 6H_2O$, and $KClO_4$. The AE signals generated from this $KClO_4$ are compared with those from a different sample reported in the previous paper.[3]

AE and DTA Apparatus

A scheme of the experimental apparatus for the simultaneous AE and DTA technique is shown in Fig. 1. This apparatus is divided into three systems, namely, the reaction system and DTA and AE systems. A schematic diagram of the sample (reference) holder covered with a cap is illustrated in Fig. 2.

Reaction System. Two fused silica holders of the same size (15 mmϕ×15 mm), covered with the cap, are placed symmetrically in a vertical electric tube furnace. As shown in Fig. 2, there are four holes on the top of the cap and three holes at its side which allow gases formed in the holder to

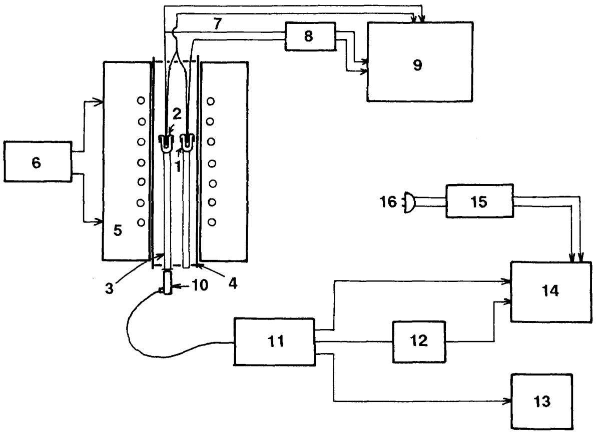

Fig. 1. A schematic diagram of experimental apparatus for simultaneous AE–DTA measurement. 1: reference holder, 2: sample holder, 3: waveguide, 4: protective silica tube, 5: electric furnace, 6: PID controller, 7: thermocouple, 8: micro-volt meter, 9: two-pen recorder, 10: sensor, 11: AE tester, 12: universal counter, 13: digital storagescope, 14: two-pen recorder, 15: noise filter, 16: electric power source.

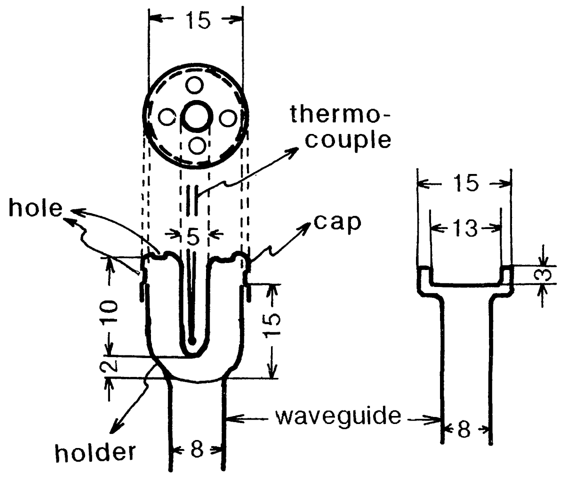

Fig. 2. Fused silica sample (reference) holder fitted with a cap (left) and a flat-bottom type sample holder (right).

escape. A 10 mm length tube of 5 mm diameter, in which the chromel–alumel thermocouple is put, is fixed downward at the center of the cap. The distance between the tube tip and the holder bottom is 2 mm. The super Kantal wound furnace is heated with a PID-program controller to avoid switching noise by an on/off controller. A protective silica tube is inserted into the furnace. All the experiments were performed at a heating rate of 5 °C min^{-1} in air. A flat bottom sample holder (13 mmϕX3 mm) was also designed for a small amount of powder sample or crystals (Fig. 2); when this holder is used, the DTA curve cannot be obtained.

DTA System. The thermocouples are placed in the cap tube of the reference and sample holders (Fig. 2) and are fixed not to move above the furnace. α-Al_2O_3 powder is used for the reference material. The temperature difference (ΔT) between the reference and sample holders is measured after amplification by a micro-volt meter and the reference temperature is simultaneously recorded.

AE System. A fused silica rod (8 mmϕ ×150 mm), fixed at the bottom of the sample holder, is used as the waveguide for AE signals (see Fig. 2). About 5 cm of the rod protrudes from the furnace and is tightly clamped. The end of the rod is polished smoothly. A 140 KHz resonance frequency piezoelectric sensor (8 mm diameter) of a single-end type brings contact with the smooth end of the rod with silicon grease. The elastic waves generated in the sample are transmitted through the waveguide rod to the sensor, where they are converted to electric signals in the form of voltage amplitude-time traces. By use of an AE TESTER (NF Electronic Instrument, 9501), the traces are discriminated at preselected levels of voltage (designated as the threshold). Such discriminated traces are observed as the complex waves by a digital storagescope (Iwatsu, model DS-6411 C) and are stored on a memory card. The envelope of each discriminated wave is electronically squared and counted as a single event count pulse. The number of the pulses counted at a time interval of 1 sec is recorded as the event count rate (cps); in this case, a dead time of 1 ms is preset. The cumulative event count is simultaneously monitored by a universal counter (Advantest, model TR 5822).

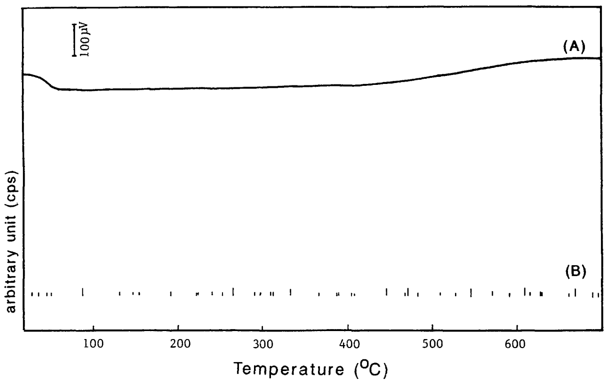

Fig. 3. The AE-DTA curve for a blank test. (A): DTA curve, (B): AE count rate curve.

Table 1. Typical Experimental Condition for AE-DTA Measurement

DTA measurement	Sample, 100—800 mg
	Reference material, α-Al_2O_3
	Heating rate, 5 °C min^{-1}
AE measurement	Threshold, 250 μV
	Count rate, 500 cps/full scale
	Recorder range, 50 mV

The elastic waves are finally displayed as three out-put parameters, the wave form, the event count rate and the cumulative event count. Much attention must be given to avoid interfering noises arising from external mechanical, electromagnetic, or vibratory sources. The induced noise caused by the PID controller is eliminated by a noise filter; the electric power passed through the filter is used for the recorder. Even so, the unfiltered noise occurs or the electrical noise can be directly picked up by the sensor from the surroundings. Such electrical noise occurs as high frequency pulse signal which is distinguished from the AE signal by observation of the digital storagescope. Figure 3 shows the result of a blank AE and DTA measurement; for the former measurement, the empty sample holder with the cap was used. The baseline of the DTA curve is found to be relatively smooth during the measurement. The discrete and irregular signals seen on the AE curve were judged as noise by the storagescope, and this defines the background noise level. A satisfactory signal to noise ratio was found to be obtained with a threshold of 250 μV from the preliminary blank tests. Typical experimental conditions for the AE and DTA measurement are listed in Table 1. No change in the noise configuration was found even when the flat bottom sample holder was used.

Samples. Five samples used were NaN_3, KNO_3, $CaCrO_4\cdot0.1H_2O$, $MgCl_2\cdot6H_2O$ (these four samples are supplied from Kanto Chem. Co., Ltd.) and $KClO_4$ (Wako Chem. Co.,Ltd.). Sample weights of 100 to 800 mg were used. The samples of $MgCl_2\cdot6H_2O$ and $CaCrO_4\cdot0.1H_2O$ were ground for 10 min in a mortar and pestle.

Results and discussion

Decomposition of NaN_3. Figure 4 shows the AE and DTA curve for the decomposition of NaN_3; the

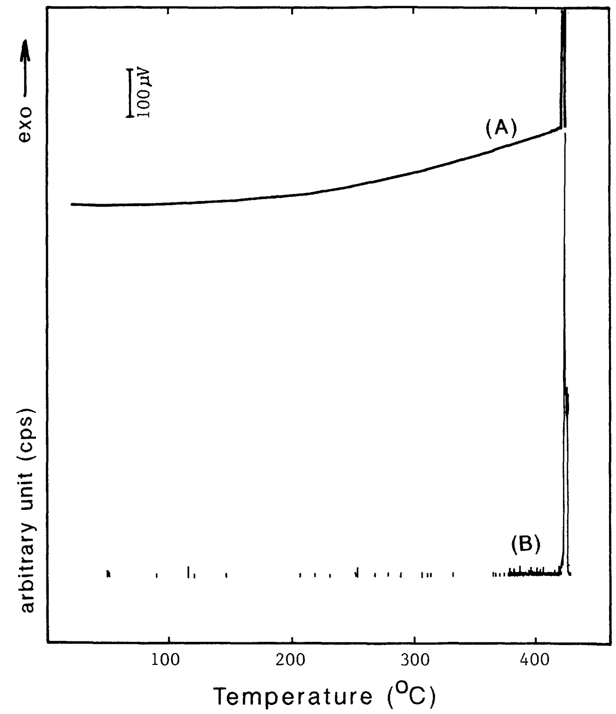

Fig. 4. The AE-DTA curve for the decomposition of NaN_3. (A): DTA curve, (B): AE count rate curve, Sample weight: 260 mg.

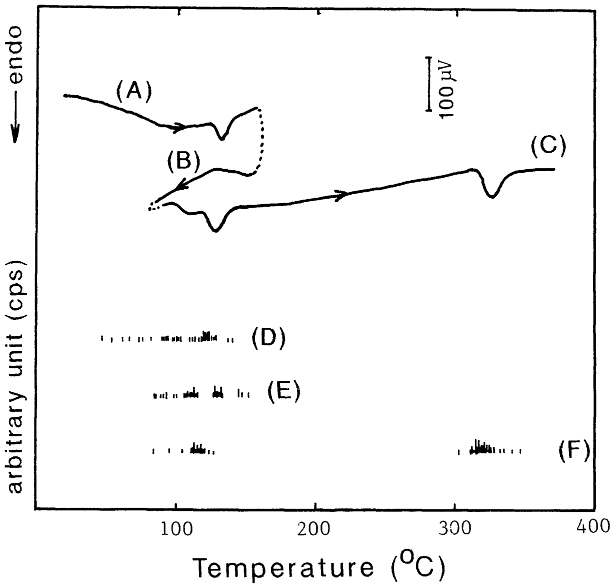

Fig. 5. The AE-DTA curve for the phase transition and melting of KNO_3. The DTA curves A, B, and C correspond to the first heating to 160 °C, followed by cooling to 80 °C, then reheating to 370 °C. The AE count rate curves D, E, and F correspond to the DTA curves A, B, and C, respectively. Sample weight: 101 mg.

samples were slightly ground to break up the aggregated particles. The DTA curve shows that the reaction proceeds explosively with a sharp exothermic peak at 422 °C, which arises from the reaction: $2NaN_3=2Na+3N_2$. The whole exothermic peak was too large to be recorded in the range preset. Sharp AE signals appear at the corresponding temperature of the explosive exothermic DTA peak. It is interesting to note that the AE signals begin 40 °C lower than the sharp decomposition DTA signal, suggesting that some mechanical change has already taken place in the particles of NaN_3, prior to the explosion.

Phase Transition of KNO_3. It has been shown by the previous DTA results that the endothermic peak due to the α to β phase transition appears at 130 °C and the melting of KNO_3 at 335 °C.[4] Figure 5 shows the AE-DTA curve of the KNO_3 sample which was obtained by heating according to the continueous heating-cooling-reheating schedule, as indicated by the arrows on the DTA curve. An unground 101 mg sample was used. The DTA curves of A to C correspond to an initial heating to 160 °C, followed by cooling to 80 °C, and reheating to 370 °C. The endothermic peak at 130 °C on DTA curve A is due to the transition of KNO_3 from the α to β phase. Although it is reported that when the β phase is cooled, the phase transition from β to γ and γ to α occurs at 124 °C and 110 °C, respectively,[5] no thermal changes are seen on curve B, probably because the natural uncontrolled cooling rate from 160 to 80 °C is too slow to give DTA signals (<1 °C min^{-1}). On reheating the α phase sample thus obtained, as shown on curve C, the $\alpha\rightarrow\beta$ phase transition again occurs at 127 °C and the KNO_3 melts at 330 °C. The AE chart sequences of D to F correspond to the DTA curves of A to C, respectively. It is seen from the AE traces that on initial heating (trace D), the AE signals due to the $\alpha\rightarrow\beta$ transition appear, the initiation temperature (around 100 °C) being lower than that of the endothermic peak (124 °C). On cooling this sample (trace E), the AE signals emitted by the $\beta\rightarrow\gamma$ and $\gamma\rightarrow\alpha$ transitions are apparently detected at temperatures of 132—125 °C and 117—105 °C, respectively, although no thermal changes appear on the DTA curve. On reheating (trace F), the observed AE signals are due to the α to β transition and the melting of KNO_3.

Phase Transition and Decomposition of $KClO_4$. Figure 6 shows the AE-DTA curve (A to C) for the phase transition and decomposition of $KClO_4$. An unground sample (600 mg) used here was supplied from the different source from that reported in our previous paper.[3] The reported DTA results have shown the endothermic peak at 303 °C, due to the transition from the orthorhombic to cubic form, and the endothermic/exothermic peaks at 580—620 °C, due to the melting and decomposition of $KClO_4$.[6] As shown in Fig. 6-C, this sample gives rise to one broad AE peak at temperatures of 200—340 °C and three sharp AE peaks (a to c) at 560—660 °C, but does not emit any AE signals below 200 °C, as was observed in

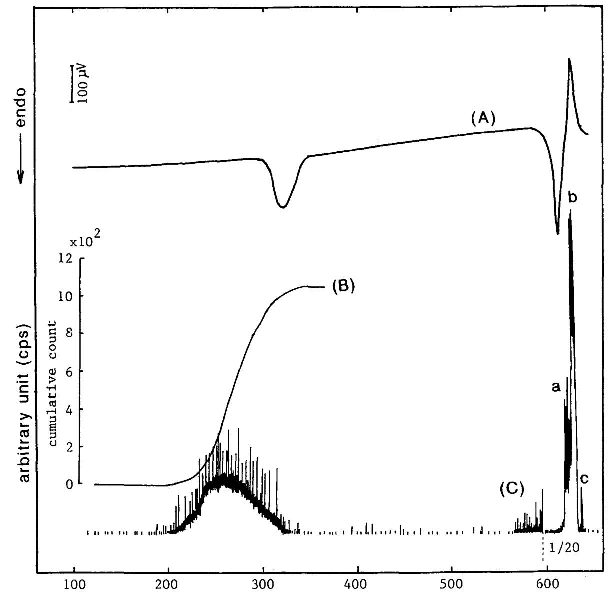

Fig. 6. The AE-DTA curve for the phase transition and decomposition of $KClO_4$. (A): DTA curve, (B): AE cumulative count curve, (C): AE count rate curve. The threshold is raised to 500 µV from the temperature corresponding to the dashed line, the intensity being reduced to 1/20. Sample weight: 600 mg.

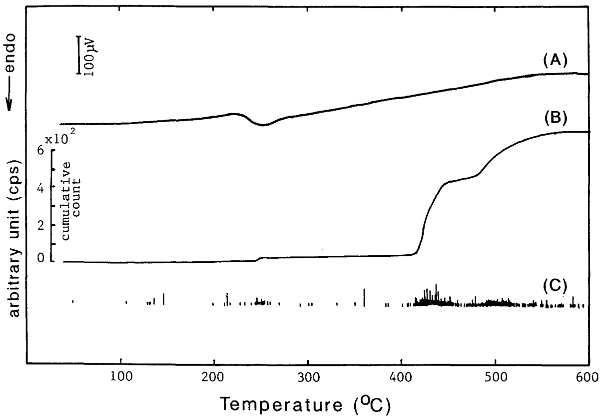

Fig. 7. The AE-DTA curve obtained on heating the $CaCrO_4 \cdot 0.1H_2O$ sample. (A): DTA curve, (B): AE cumulative count curve, (C): AE count rate curve, Sample weight: 800 mg.

the $KClO_4$ previously studied. Since the initiation temperature of the broad AE peak (200 °C) is much lower than that of the endothermic DTA peak due to the transition (300 °C), this AE peak suggests occurrence of some mechanical change in the particles prior to the transition. A slight increase in the cumulative count curve at around 300 °C indicates the addition of the AE signals due to the transition to those by the mechanical change occurring before the trasition above 300 °C. The high temperature AE peaks a and b correspond to the endothermic peak at 620 °C and the exothermic peak at 632 °C, respectively, which are due to the melting of $KClO_4$ and its subsequent decomposition. Peak a begins at 565 °C, lower than the onset temperature of melting (590 °C). Peak b begins at the inflexion temperature of the endothermic/exothermic peak; the threshold value was raised at temperatures above 597 °C, reducing the intensity to about 1/20. As was mentioned in the previous paper,[3] two intense peaks a and b suggest two step decomposition of the molten $KClO_4$; the early part of peak a contains the AE signals due to melting. Peak c results from the solidification of the molten decomposition product KCl, which is not detected by DTA.

Dehydration of $CaCrO_4 \cdot 0.1H_2O$. Figure 7 shows the AE-DTA curve (A to C) obtained on heating a ground sample of $CaCrO_4 \cdot 0.1H_2O$ to 600 °C. The molecular weight of water ($0.1H_2O$) in the sample was determined by TG-DTA apparatus (Rigaku thermoflex 8100 type), since this sample was labelled $CaCrO_4 \cdot x\text{-}H_2O$. The TG result showed a small weight decrease (about 1 wt%) at 230—320 °C, continuing sluggishly at 330—560 °C (about another 1 wt%). On the DTA curve, a small endothermic peak appears at 235—280 °C, above which no thermal change is seen. This endothermic peak is probably due to the dehydration of $0.1H_2O$, since the temperature range of this peak corresponds to that of the low temperature weight loss monitored by TG. It is seen from the AE count rate curve that the signals are generated in two temperature regions, 245—260 °C and 410—590 °C. The latter region occurs in two stages, at is indicated by two step in the cumulative count curve. The low temperature signals are probably caused by the dehydration. The signals occurring in two stages at high temperatures above 390 °C are associated with the second sluggish weight loss, but their origin is not clear at prsent, since neither the yellow color nor the X-ray diffraction pattern of the sample changes as a result of the heating.

Dehydration of $MgCl_2 \cdot 6H_2O$. Figure 8 shows the AE-DTA curve obtained on heating a ground sample of $MgCl_2 \cdot 6H_2O$ to 500 °C. Since the powders of $MgCl_2 \cdot 6H_2O$ are hygroscopic, the crystalline samples were ground in a dry nitrogen atmosphere. As has been reported previously,[7] six endothermic peaks a to f at 126, 180, 207, 229, 273, and 445 °C, respectively, are assigned as follows; a: melting of $MgCl_2 \cdot 6H_2O$, b: $MgCl_2 \cdot 6H_2O = MgCl_2 \cdot 4H_2O + 2H_2O$ c: $MgCl_2 \cdot 4H_2O = MgCl_2 \cdot 2H_2O + 2H_2O$, d: $2MgCl_2 \cdot 2H_2O = MgCl_2 \cdot H_2O + MgOHCl + 2H_2O + HCl$, e: $2MgCl_2 \cdot H_2O = MgCl_2 + MgOHCl + H_2O + HCl$, f: $MgOHCl = MgO + HCl$. Since the AE signals appearing at 50—60 °C are not accompanied by any thermal effect, they are probably due to the liberation of moisture absorbed on the particles on heating. The signals are again seen from the peak temperature of a, corresponding to melting of $MgCl_2 \cdot$

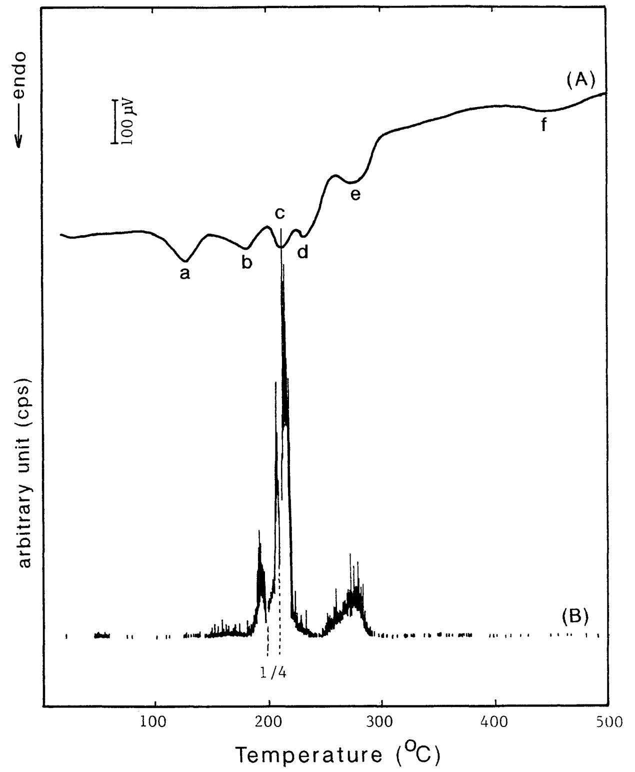

Fig. 8. The AE–DTA curve for the dehydration of $MgCl_2\cdot 6H_2O$. The threshold is raised to 350 μV between the dashed lines, the intensity being reduced to 1/4. (A): DTA curve, (B): AE count rate curve, Sample weight: 160 mg.

$6H_2O$, and continue to 185 °C at which the $2H_2O$ is dehydrated. They intensify over the temperature region corresponding to the dehydration of $2H_2O$ from $MgCl_2\cdot 4H_2O$ (peak c). They decrease over the temperature range of peak d and appear again as relatively intense AE signals of high amplitude, occurring over the range of peak e. These signals are associated with bubbling of the molten sample, as is indicated by the presence of many blowholes and bubbles in the sample after the experiment. Then, the AE signals intermittently occur up to about 400 °C, above which they cease altogether.

From the results described above for NaN_3, KNO_3, $KClO_4$, $CaCrO_4\cdot 0.1H_2O$, and $MgCl_2\cdot 6H_2O$, the AE technique has proved to be very useful and sensitive method for following the changes taking place in the inorganic salts in the course of heating. For example, the decomposition of $KClO_4$ in molten phase, which has been judged as one step process by DTA or TG , was thought to occur as two step process from the doublet of AE curve. Thus, the authors expect that the AE is used as a new thermoanalytical technique complementing DTA, TG, and other technique.

References

1) R. V. Williams, "Acoustic Emission," Adam Hilger Ltd., Bristol (1980), p. 1.

2) K. Lønvik, *Thermochim. Acta,* **110**, 253 (1987).

3) S. Shimada and R. Furuichi, *Thermochim. Acta,* in press.

4) E.S. Freeman and D. Edelman, *Anal. Chem.,* **31**, 624 (1959).

5) "Rikagaku Jiten," ed by F. Tamamushi, et al., Iwanami Shoten, Tokyo (1971), p 636.

6) M.M. Markowitz and D.A. Boryta, *J. Phys. Chem.,* **69**, 1114 (1965).

7) S. Shimada, R. Furuichi, and T. Ishii, *Kogyo Kagaku Zasshi,* **74**, 2006 (1971).